Vol. 82, No. 22

Early B-Cell Activation after West Nile Virus Infection Requires Alpha/Beta Interferon but Not Antigen Receptor Signaling[▽]

Whitney E. Purtha,[1] Karen A. Chachu,[1] Herbert W. Virgin IV,[1] and Michael S. Diamond[1,2,3]*

Pathology & Immunology,[1] Medicine,[2] and Molecular Microbiology,[3] Washington University School of Medicine, St. Louis, Missouri 63110

The B-cell response against West Nile virus (WNV), an encephalitic *Flavivirus* of global concern, is critical to controlling central nervous system dissemination and neurological sequelae, including death. Here, using a well-characterized mouse model of WNV infection, we examine the factors that govern early B-cell activation. Subcutaneous inoculation with a low dose of replicating WNV results in extensive B-cell activation in the draining lymph node (LN) within days of infection as judged by upregulation of the surface markers CD69, class II major histocompatibility complex, and CD86 on CD19+ cells. B-cell activation in the LN but not the spleen was dependent on signals through the type I alpha/beta interferon (IFN-α/β) receptor. Despite significant activation in the draining LN at day 3 after infection, WNV-specific B cells were not detected by immunoglobulin M enzyme-linked immunospot analysis until day 7. Liposome depletion experiments demonstrate that B-cell activation after WNV infection was not affected by the loss of F4/80+ or CD169+ subcapsular macrophages. Nonetheless, LN myeloid cells were essential for control of viral replication and survival from infection. Overall, our data suggest that the massive, early polyclonal B-cell activation occurring in the draining LN after WNV infection is immunoglobulin receptor and macrophage independent but requires sustained signals through the type I IFN-α/β receptor.

B cells have a critical role in protection against viral infections. Although classically considered part of the adaptive immune response, B cells are activated soon after infection by several viruses prior to the generation of specific immunoglobulin G (IgG) (6, 13). While many groups have focused on defining the immunologic events that govern induction or perpetuation of the adaptive B-cell humoral response, the mechanisms that regulate the early stage of activation remain poorly characterized.

Although not completely understood, the early B-cell activation response may contribute to production of natural antibody (36), the induction of memory B-cell populations (5), or the retention of cells in lymphoid organs (47). Several groups have recently investigated the kinetics and requirements for B-cell activation after virus infection in mice. Rotavirus infection promoted substantial T-cell-independent B-cell activation by day 3 in the mesenteric lymph nodes (LN) in wild-type mice (6, 7). Polyclonal B-cell activation and virus-specific antibody responses against influenza virus were dependent on type I interferon (IFN) signaling (11, 13). In contrast, B-cell activation of mediastinal LN after murine gammaherpesvirus 68 infection was delayed until day 10 and required T-cell help (52). In general, the specific signaling pathways, cellular requirements, and the cell subsets involved in the early B-cell response and their functional consequences have not been fully established.

The B-cell response to viruses is often initiated in draining and secondary LN when naïve B cells recognize antigen via their surface immunoglobulin receptor. B cells in the circulation enter the LN via high endothelial venules and localize to the follicular region, where antigen encounters occur. Activated B cells then migrate to T-cell parafollicular areas to receive instructive signals to proliferate, differentiate, and produce antibodies. Viral antigens can traffic into B-cell follicles as either soluble or cell-associated antigen through afferent lymphatic vessels (10). Soluble viral antigen may diffuse across the subcapsular sinus through small gaps, although this is limited to low-molecular-weight proteins (38). Viral antigen also may be translocated and presented to B cells by resident CD169+ macrophages that line the subcapsular sinus (9, 25, 39). Alternatively, migratory dendritic cells, which are infected or display viral antigen on their surface, may directly present or cross-present to B cells (41).

West Nile virus (WNV) is a neurotropic flavivirus that is now the leading cause of epidemic encephalitis in North America (45). Mouse models of WNV infection have elucidated the stages of pathogenesis, kinetics of dissemination, tropism, and immune system elements that restrict lethal infection (reviewed in reference 43). After mosquito inoculation in the skin, WNV is believed to infect subsets of dermal dendritic cells (8), which migrate to the draining LN, where the innate immune response is amplified and the adaptive immune response is initiated. In particular, B cells and antibody have essential functions during the early stages of WNV infection. Mice deficient in B cells develop increased viral burden in serum and uniformly succumb to infection (17). The early IgM response, in part, limits viral dissemination, as low titers of anti-WNV IgM antibodies at day 4 predict mortality (18). Moreover, passive transfer of serum containing WNV-specific IgM protected secretory IgM−/− recipient mice from lethal

* Corresponding author. Mailing address: Departments of Medicine, Molecular Microbiology and Pathology & Immunology, Washington University School of Medicine, 660 South Euclid Avenue, Box 8051, St. Louis, MO 63110. Phone: (314) 362-2842. Fax: (314) 362-9230. E-mail: diamond@borcim.wustl.edu.

infection. Given the importance of the early IgM response to protection against WNV in mice, here we analyzed the initial steps of B-cell activation after infection. We observed considerable early B-cell activation in the draining LN within 48 to 72 h after WNV infection, and this process required sustained signaling through the type I IFN-α/β receptor. Notably, early B-cell activation after WNV infection was polyclonal, immunoglobulin receptor independent, and did not require the presence of CD169+ subcapsular macrophage to process viral antigen.

MATERIALS AND METHODS

Virus stocks and infection. The WNV strain 3000.0259 (WNV-NY) was isolated from mosquitoes in New York in 2000 (19) and passaged once in C6/36 *Aedes albopictus* cells, and titers were determined on BHK21-15 cells. Virus (5×10^7 PFU/ml) was diluted to 10^2 PFU in 50 μl in Hanks balanced salt solution with 1% heat-inactivated fetal bovine serum (FBS) for subcutaneous injection into mice via the footpad. WNV strain Madagascar-AnMg798 (WNV-MAD) was obtained from the World Reference Center of Emerging Viruses and Arboviruses and passaged analogously. Murine norovirus (MNV) strain MNV1.CW3 was used for all norovirus infections (55). To generate a concentrated norovirus stock, RAW 264.7 cells were infected in VP-SFM medium (Gibco) for 2 days at a multiplicity of infection of 0.05. Supernatants were clarified by low-speed centrifugation for 20 min at 3,000 rpm. Virus was concentrated by centrifugation at 4°C for 3 h at 27,000 rpm ($90,000 \times g$) in an SW32 rotor. Viral pellets were resuspended in phosphate-buffered saline (PBS), and titers were determined on RAW 264.7 cells as previously described (55). Mice were infected perorally with 3×10^7 PFU of MNV. The mock control was defined as subcutaneous or peroral inoculation with an equivalent volume of the vehicle (Hanks balanced salt solution and 1% heat-inactivated FBS).

Mice. Wild-type C57BL/6 mice were obtained commercially (Jackson Laboratories, Bar Harbor, ME). Congenic deficient C57BL/6 mice were obtained from colleagues, as follows: IRF-3$^{-/-}$ and IRF-7$^{-/-}$ (24, 44), gifts of T. Taniguchi (University of Tokyo); Myd88$^{-/-}$ (1), gift of M. Colonna (Washington University); TLR3$^{-/-}$ (2), gift of R. Flavell (Yale University); IFN-α/β receptor (IFN-α/βR)$^{-/-}$, gift of J. Sprent (Scripps Institute); C3$^{-/-}$ (12), gift of H. Molina (Washington University). The following mice were purchased commercially: IFN-γ$^{-/-}$ (15), IL-6$^{-/-}$ (27), and *RAG* T- and B-cell-deficient mice (35), all from Jackson Laboratories (Bar Harbor, ME); major histocompatibility complex (MHC) class II$^{-/-}$ (32), Taconic (Germantown, NY). All deficient mice were genotyped and bred in the animal facility of Washington University School of Medicine. The HELMET mice are MD4 Hen egg lysozyme (HEL) transgenic mice on the B6.129S2-*Igh-6^{tm1Cgn}* background (also referred to as B-cell$^{-/-}$ μMT mice). The presence of HEL-specific B cells was confirmed by flow cytometric analysis of peripheral blood using allotype-specific antibodies to IgM as described previously (33). All experiments used mice 8 to 12 weeks of age and were performed in accordance with Washington University Animal Studies guidelines.

Flow cytometry analysis and antibodies. Inguinal, popliteal, and mesenteric LN and spleens were dissected from mock- or virus-infected mice. Single-cell suspensions were generated in Dulbecco's modified Eagle's medium containing 10% FBS. After erythrocyte lysis with ACK buffer (0.15 M NH$_4$Cl, 10 mM KHCO$_3$, 0.1 mM Na$_2$EDTA, pH 7.2), cells were counted by hemocytometry, washed with PBS supplemented with 5% normal goat serum (PBS-NGS), and incubated with conjugated antibodies. The following antibodies against mouse antigens and secondary conjugates were purchased from BD Biosciences (San Jose, CA): anti-CD4–allophycocyanin (APC; RM4-5), anti-CD8α–APC (53-6.7), anti-CD11b–APC (M1/70), anti-CD11c–phycoerythrin (PE; HL3), anti-CD19–APC (1D3), anti-CD21–PE (7G6), anti-CD23–biotin (B3B4), anti-CD86–PE (GL1), anti-IgD–PE (11-26c.2a), anti-CD69–fluorescein isothiocyanate (FITC; H1.2F3), anti-CD5–PE (53-7.3), anti-IgM–biotin (II-41), and streptavidin–APC-Cy7. Anti-CD169–FITC (3D6.112) was obtained from AbD Serotec (Oxford, United Kingdom), anti-F4/80–FITC (BM8) was from eBioscience (San Diego, CA), and biotin-conjugated anti-I^E/I^A was obtained from Invitrogen (Carlsbad, CA). Cells were stained in PBS-NGS to minimize nonspecific binding, and appropriate isotype control antibodies purchased from BD Biosciences were used. Data were collected on BD FACScalibur or FACSArray flow cytometers and analyzed using FlowJo software (Treestar, Inc., Ashland, OR). A commercially available kit was used to measure intracellular staining of Ki-67 (BD Bioscience). For antibody blockade of the IFN-α/βR, 1 mg of MAR1-5A3 (46)

was administered to mice via intraperitoneal injection at specified times relative to WNV infection.

Measurement of antigen-specific B cells. WNV antigen-specific B cells were identified by an enzyme-linked immunospot (ELISPOT) assay after modification of published protocols (20, 51). Microtiter filter plates with mixed cellulose ester membranes (Millipore, Billerica, MA) were incubated overnight at 4°C with 40 μg/ml of purified, recombinant WNV envelope (E) protein (37) or ovalbumin diluted in PBS. Membranes were washed with PBS with 0.1% Tween 20 (PBS-T) and blocked for 1 hour at room temperature with complete medium (Dulbecco's modified Eagle's medium supplemented with 10% FBS, penicillin-streptomycin, 1 mM sodium pyruvate, 0.1 mM nonessential amino acids, 10 mM HEPES, and 50 μM β-mercaptoethanol). LN cells were isolated, suspended in complete RPMI medium, and added to 96-well microtiter plate at 10^6 cells per well with serial threefold dilutions. Cells were incubated on the membranes for 5 hours at 37°C in 5% CO$_2$. Subsequently, plates were washed twice with PBS and twice with PBS-T and incubated overnight at 4°C with biotinylated anti-IgM (1 μg/ml in PBS-T supplemented with 1% FBS). Following washing, horseradish peroxidase (HRP)-conjugated streptavidin (5 μg/ml) was added to wells for 1 hour at room temperature and plates were washed with PBS. Chromogen substrate (3-amino-9-ethyl-carbozole; Sigma-Aldrich) was added to develop spots, and reactions were quenched after rinsing with water. Spots were counted using a binocular microscope (Olympus SZX7; 20× magnification).

Serological analysis. An enzyme-linked immunosorbent assay was used to measure WNV-specific antibody titers as described previously (37). Briefly, recombinant WNV E ectodomain protein (5 μg/ml in 0.1 M sodium carbonate buffer [pH 9.3]) was adsorbed on 96-well Maxi-sorp microtiter plates (Nalge Nunc, Rochester, NY) overnight at 4°C. Plates were washed and blocked with PBS-T with 5% bovine serum albumin for 1 hour at 37°C. Serum from naïve or WNV-infected mice was diluted serially in PBS-T and added to plates for 1 hour at 37°C. After washing four times with PBS-T, biotin-conjugated goat anti-mouse IgG, IgG1, IgG2b, IgG2c, IgG3, or IgM (1 μg/ml in PBS-T; 1 hour at room temperature) and streptavidin-conjugated horseradish peroxidase (2 μg/ml in PBS-T; 1 hour at room temperature) were added sequentially. After a final series of washes, plates were developed with tetramethylbenzidine substrate and quenched after addition of 1 N H$_2$SO$_4$. Subsequently, the optical density at 450 nm (OD$_{450}$) was measured and adjusted for background by subtracting the OD$_{450}$ of blocked control wells. Best-fit lines were calculated, and endpoint titers were determined as 3 standard deviation units above the background signal by using Prism 4 (GraphPad Software Inc., San Diego, CA).

Liposome preparation. Clodronate liposomes were prepared according to a published method (54). Briefly, 8 mg of cholesterol (Sigma-Aldrich) and 86 mg of phosphatidyl choline (Sigma-Aldrich) were dissolved in 10 ml of chloroform. Excess chloroform was evaporated and then removed under vacuum. Clodronic acid disodium salt (Cl$_2$MDP; Sigma-Aldrich) was dissolved in deionized water and the pH adjusted to 7.3 with 5 N NaOH. The dry lipid pellet was resuspended in either 2.5 g of Cl$_2$MDP in 10 ml of water for macrophage-depleting liposomes or PBS for control liposomes. The suspension was incubated at room temperature for 2 hours to allow liposome swelling and then sonicated in a water bath for 3 minutes and stored at 4°C overnight. After centrifugation (10,000 × g for 15 min), nonencapsulated Cl$_2$MDP or PBS was removed using a flexible catheter on a 10-ml syringe. Liposomes were washed thrice with PBS by ultracentrifugation (Beckman L-80 ultracentrifuge with 70.1 Ti rotor; 22,000 × g for 30 min) and resuspended in a final volume of 4 ml of PBS. To confirm that clodronate-containing lipsomes effectively depleted macrophages, C57BL/6 *RAG*$^{-/-}$ mice were injected intravenously with 0.1 ml of liposome suspension intravenously and splenocytes were analyzed by flow cytometry 24 h later for expression of F4/80, CD11b, and CD11c markers. For depletion of macrophages in the draining LN, mice were subcutaneously injected with 50 μl of liposome suspension in each footpad 7 days prior to WNV infection according to published protocols (25).

Quantification of viral burden. WNV burden from homogenized tissues or serum was determined by plaque assay on Vero cells as previously described (17).

WNV RVPs and neutralization assays. Neutralization assays were performed as previously described (40). Briefly, to produce WNV reporter virus particles (RVPs), BHK cells that propagate a green fluorescent protein (GFP)-expressing lineage 2 WNV replicon were transfected with the structural genes of WNV-NY. Supernatant containing RVPs was collected 48 h after transfection. For RVP neutralization experiments, 10 serial fourfold dilutions of mouse serum samples were added to a 96-well plate in duplicate. Diluted RVPs were incubated with serum samples for 1 h at room temperature. The RVP-serum mixture was added to wells containing human Raji B cells (5×10^4) that transgenically express the WNV attachment ligand DC-SIGNR. After 48 h, cells were harvested and analyzed for RVP infection by flow cytometry. Data were fit to a variable slope, and 50% effective concentration values were predicted by a nonlinear regression.

RESULTS

Early activation of B cells after WNV infection. Previous studies had demonstrated that the early IgM response restricts WNV dissemination to the central nervous system (17, 18). However, it remained unclear how and when B cells become activated after WNV infection. To begin to address this, we performed a kinetic analysis of B-cell activation by using CD69 expression as a marker of early activation (31) in the draining ipsilateral inguinal LN (ILN) after footpad inoculation with 10^2 PFU of a virulent North American WNV strain (WNV-NY). Induction of CD69 on CD19$^+$ B cells was detected within 2 days, and remarkably, nearly 70% of CD19$^+$ B cells expressed this marker by 3 days after WNV-NY infection (Fig. 1A; see also Fig. 3E, below). Notably, CD69 expression on CD19$^+$ B cells was transient and rapidly downregulated to baseline levels within 6 days of infection. In comparison, activation of T-cell subsets was less prominent, as ~40% of CD4$^+$ and CD8$^+$ T cells became activated within the initial 4 days of infection (Fig. 1C and D). B-cell activation required replicating infectious WNV-NY, as mice infected with equivalent or higher (5×10^5 PFU) amounts of formalin-fixed virus showed no change in surface expression of CD69 (data not shown). Early B-cell activation after infection corresponded with an increase in the total number of CD19$^+$ B cells in the ILN, as by day 4 B-cell numbers were ~4-fold higher (Fig. 1B) ($P < 0.0001$). Similar results were observed in the draining ipsilateral popliteal lymph node; moreover, and as expected, a delay in B-cell activation was observed in the contralateral draining lymph nodes, which requires hematogenous spread of viral infection (Fig. 1I).

To determine if this increase was due to the proliferation of resident ILN B cells or an influx of B cells from other systemic compartments, we analyzed expression of the proliferation-associated nuclear antigen Ki-67. Ki-67 is exclusively expressed during all stages of the cell cycle except G_0 and is a reliable marker for identifying proliferating lymphocytes (22). Based on Ki-67 staining, B cells in the ILN after WNV-NY infection were no more proliferative than naïve B cells (Fig. 1E); in contrast, stimulation of B cells with a positive control mitogenic signal (CD40 and interleukin-4 [IL-4]) induced a distinct Ki-67 expression pattern. Thus, within a few days of WNV infection, B-cell hyperplasia in the draining lymph node is likely due to an accumulation of circulating B cells that become rapidly activated and retained.

To determine whether the robust early B-cell activation phenotype was specific for the draining LN, we also analyzed B cells in the spleen. As judged by acquisition of CD69 expression, splenic CD19$^+$ B cells were less activated (18%) relative to ILN B cells (65%), and peak activation was delayed kinetically until 4 days after WNV-NY infection (Fig. 2A). Also analogous to the ILN data, smaller subsets of T cells in the spleen were activated and, again, this occurred at a slightly later time point in comparison to B cells (Fig. 2C and D). The absolute number of B cells in the spleen expanded twofold through day 4

after infection (Fig. 2B), and this increase also was not due to proliferation of resident splenic B cells (Fig. 2E).

Because a large percentage of ILN B cells expressed CD69 after WNV infection, we hypothesized that activation may not depend on triggering or recruitment of antigen-specific B cells. To address this, we measured B-cell activation after WNV-NY infection in transgenic mice that express a single B-cell receptor specific for hen egg lysozyme (HELMET mice). Similar to wild-type mice, HELMET mice showed a high percentage of CD69$^+$ B cells 3 days after WNV infection (Fig. 1H). This experiment confirmed that the early stage of B-cell activation in response to WNV infection does not depend on antigen-specific triggering through the surface immunoglobulin receptor.

To confirm that increased CD69 expression on B cells after WNV-NY infection reflected a true state of activation, we assessed surface levels of class II MHC and CD86 on CD19$^+$ CD69$^+$ and CD19$^+$ CD69$^-$ cells. At 3 days after infection, LN B cells that expressed CD69 also showed elevated coexpression of class II MHC (Fig. 3A) ($P < 0.001$) and the costimulatory molecule, CD86 (Fig. 3B) ($P < 0.0001$). Thus, CD69 expression on B cells after WNV infection corresponds to an enhanced state of cellular activation, as judged by several independent surface markers.

Subset analysis of activated B cells. Within lymphoid tissues, B-cell subsets can be distinguished by the expression of specific cell surface markers. Transitional B cells express high levels of surface IgM and low levels of IgD, whereas mature B cells upregulate IgD and modestly downregulate IgM expression (23). Four days after WNV-NY infection, CD19$^+$ CD69$^+$ cells in the spleen and the LN expressed surface IgM and IgD at levels consistent with a mature B-cell phenotype (Fig. 3F and data not shown). In the spleen, B-cell localization has implications for specific function: follicular (CD21^{high} CD23^{high}) B cells produce antibody after instruction by T helper cells, and marginal zone (CD21^{high} CD23^{low}) B cells respond rapidly to pathogens in a T-cell-independent manner (29, 30, 53). Flow cytometric analysis revealed that WNV infection induced CD69 on the surface of both follicular (Fig. 3C and H) and marginal zone (Fig. 3C and I) B-cell subsets. Taken together, WNV infection results in the activation of B cells with several distinct functional phenotypes.

B-cell activation in the LN after infection with a murine norovirus. To establish whether the extensive B-cell activation that occurred in the draining LN was specific to WNV infection, we repeated experiments with MNV. In this case, MNV was administered orally, and the draining mesenteric LN from the gut and spleen were analyzed for B-cell activation. Remarkably, despite the differences in viral family (*Flaviviridae* versus *Caliciviridae*) and route of inoculation (subcutaneous versus peroral), the kinetics of CD69 expression on mesenteric B cells after MNV infection were remarkably similar (Fig. 4A), with a rapid (~50%, within 2 days) yet transient activation pattern. Analogously, subsets of CD4$^+$ and CD8$^+$ T cells also expressed CD69 within a few days of infection, again to lower degrees (data not shown). In contrast to that observed with WNV-NY, CD69 expression on splenic B or T cells was not appreciably detected after MNV infection (Fig. 4B and data not shown); this was not due to differential infection, as WNV and MNV both generate similar titers of ~10^3 to 10^4 PFU/g in the spleen by days 3 to 5 (data not shown). Given the analo-
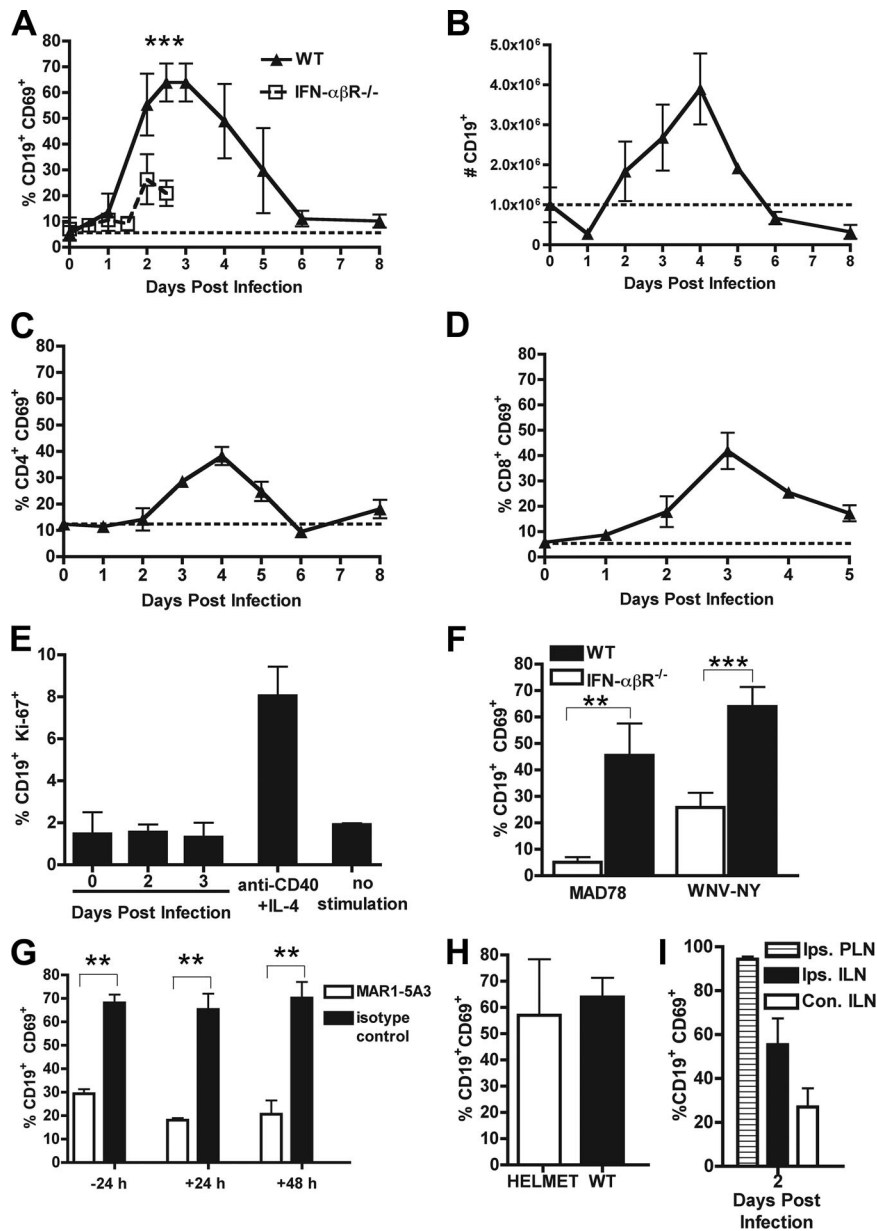
FIG. 1. B-cell activation in the draining LN. A. Expression of CD69 on CD19^{+} B cells after WNV-NY infection in wild-type (WT) and IFN-α/βR^{−/−} mice. The data reflect averages from 5 to 10 mice per time point. B. Total number of CD69^{+} CD19^{+} B cells in the ILN after WNV-NY infection. C and D. Expression of CD69 on CD4^{+} (C) and CD8^{+} (D) T cells after WNV-NY infection. E. Measurement of B-cell proliferation in ILN at the indicated days after WNV infection or mitogenic stimulus (anti-CD40 plus IL-4) as judged by Ki-67 expression. F. Expression of CD69 on CD19^{+} B cells in wild-type and IFN-α/βR^{−/−} mice 3 days after infection with WNV-MAD or WNV-NY. G. Effect of neutralizing anti-IFN-α/βR MAb (MAR1-5A3) on CD69 expression on CD19^{+} B cells after WNV infection. Mice were treated with MAb (or isotype control) at the indicated times relative to infection, and B cells were analyzed at 3 days after infection. H. Expression of CD69 on CD19^{+} B cells in HELMET mice 3 days after WNV infection. The dotted line represents the basal level of expression in naïve wild-type mice. Asterisks indicate time points at which differences are statistically significant (**, $P < 0.01$; ***, $P < 0.001$). I. Expression of CD69 on CD19^{+} B cells from the ipsilateral popliteal lymph node (PLN), ipsilateral ILN, and contralateral ILN node 2 days after WNV infection.

gous prior B-cell activation experiments with influenza virus (13) and rotavirus (6), the pattern of activation in the draining LN after WNV infection may reflect a general response to acute infection by RNA viruses.

Early B-cell activation in the ILN requires IFN-α/β signaling. As B cells are generally not permissive for WNV infection in mice (42), we hypothesized that host innate immune factors

released from infected cells in the LN would regulate the early B-cell activation response. As a previous study suggested that type I IFN-α/β modulates B-cell activation after influenza virus infection (13), we repeated infection experiments in IFN-α/βR^{−/−} mice. Notably, B cells from IFN-α/βR^{−/−} mice showed marked reductions in CD69 expression in the ILN (Fig. 1A) ($P < 0.0001$), with a peak of ~25% at day 2. In contrast, in
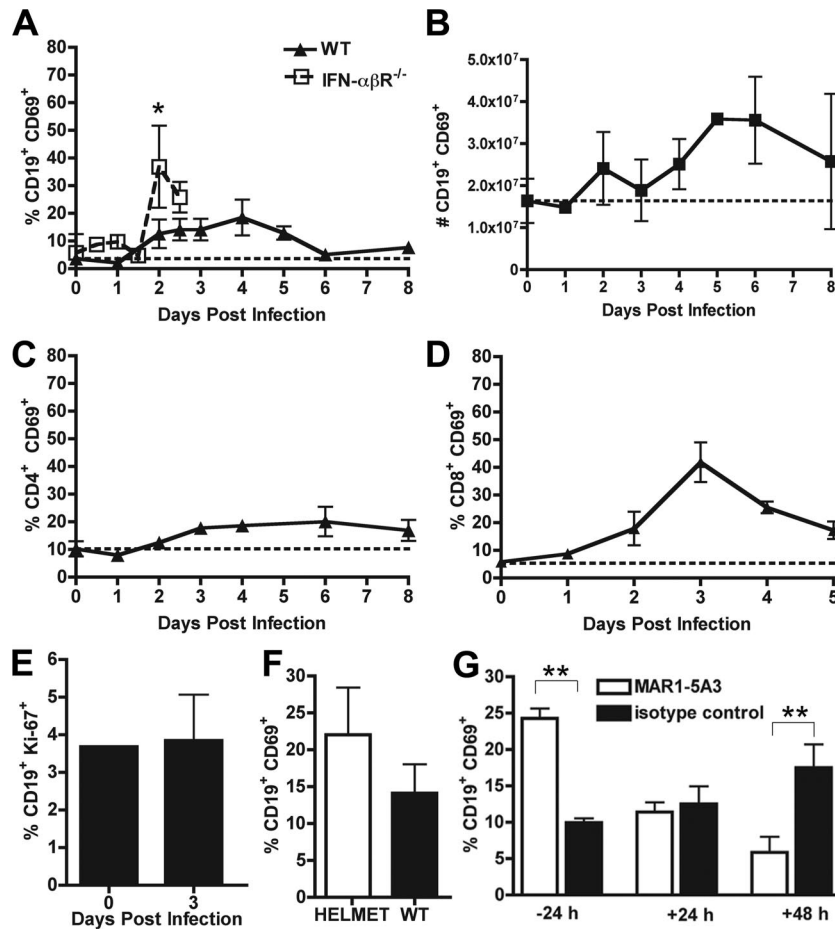
FIG. 2. B-cell activation in the spleen. A. Expression of CD69 on CD19$^+$ splenic B cells after WNV-NY infection in wild-type and IFN-α/βR$^{-/-}$ mice. The data reflect averages from 5 to 10 mice per time point. B. Total number of CD69$^+$ CD19$^+$ B cells in the spleen after WNV-NY infection. C and D. Expression of CD69 on CD4$^+$ (C) and CD8$^+$ (D) T cells after WNV-NY infection. E. Measurement of B-cell proliferation in the spleen at the indicated days before or after WNV infection as judged by Ki-67 expression. F. Expression of CD69 on CD19$^+$ B cells in HELMET mice 3 days after WNV infection. G. Effect of neutralizing anti-IFN-α/βR MAb (MAR1-5A3) on CD69 expression on splenic B cells after WNV-NY infection. Mice were treated with MAb (or isotype control) at the indicated times relative to infection, and B cells were analyzed at 3 days after infection. The dotted line represents the basal level of expression in naïve wild-type mice. Asterisks indicate time points at which differences are statistically significant (∗, $P < 0.05$; ∗∗, $P < 0.01$).

IFN-α/βR$^{-/-}$ mice, a significant increase in B-cell activation as judged by CD69 expression was observed in the spleen (Fig. 2A and G, 36% compared to 12% at day 2) ($P < 0.05$).

Because IFN-α/βR$^{-/-}$ mice die rapidly after infection with the virulent WNV-NY strain, to obtain confirmatory kinetic data we assessed CD69 expression on B cells in wild-type and IFN-α/βR$^{-/-}$ mice after infection with an attenuated lineage 2 virus, WNV-MAD; this strain shows delayed mortality in IFN-α/βR$^{-/-}$ mice compared to WNV-NY (26). Although a higher dose was required to activate comparable levels of B cells in wild-type mice, there was a similar, marked reduction (Fig. 1F) ($P < 0.01$) in B-cell activation in IFN-α/βR$^{-/-}$ mice after WNV-MAD infection.

To further understand the role of type I IFN-α/β in activating B cells in the draining LN after WNV infection, we utilized a recently characterized blocking antibody (MAR1-5A3) (46) against the IFN-α/βR. A single 1-mg dose of the MAR1-5A3 monoclonal antibody (MAb) was administered at different times relative to WNV inoculation, and CD69 expression on B

cells was monitored at day 3 after infection. Importantly, administration of equivalent amounts of an isotype control MAb had no effect on CD69 expression on B cells at any time point (data not shown). However, when anti-IFN-α/βR MAb was given 24 h before infection, CD69 expression was reduced on B cells in the ILN (Fig. 1G). Somewhat surprisingly, MAb administered 24 or even 48 h after infection also blunted CD69 expression on B cells. Thus, sustained type I IFN signaling is required for CD69 expression on B cells in the ILN after WNV infection.

As IFN-α/βR signaling was required for early CD69 expression and activation of ILN B cells, we were interested in evaluating the viral recognition pathways upstream of IFN induction that activated B cells. We measured CD69 expression on B cells from a panel of WNV-infected congenic mice that lacked individual genes associated with IFN-α/β induction after RNA virus infection (e.g., TLR3, IRF-3, IRF-7, and Myd88). Mice deficient in TLR3, which binds double-stranded RNA in the endosome, showed a small yet statistically signif-
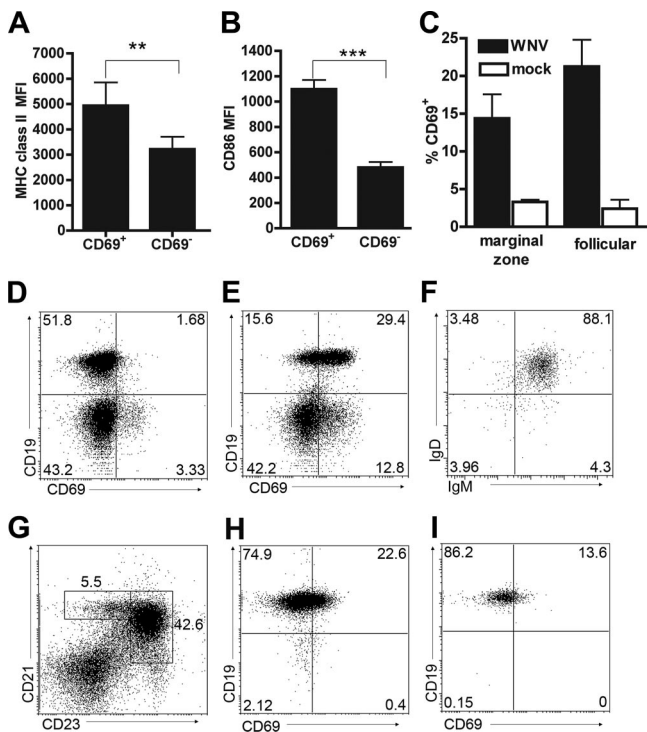
FIG. 3. Phenotyping of activated B cells in LN and spleen after WNV infection. A and B. B-cell activation in the draining LN at day 3 after WNV infection was assessed by immunostaining for increased surface expression of MHC class II (A) and CD86 (B). Three-color staining was performed with $CD19^+$ $CD69^+$ and $CD19^+$ $CD69^-$ cells. Asterisks indicate differences that are statistically significant (**, $P <$ 0.01; ***, $P < 0.001$). D and E. WNV infection induces CD69 expression on $CD19^+$ B cells. A representative flow cytometry panel of LN cells from uninfected (D) and WNV-infected (E) mice is shown. F. All of the $CD69^+$ B cells in the LN showed a mature (surface IgD^+ IgM^+) phenotype. G to I. CD69 staining on different B-cell subsets in the spleen at day 4 after WNV infection. (H and I) Follicular ($CD21^{high}$ $CD23^{high}$) (H) and marginal zone ($CD21^{high}$ $CD23^{low}$) (I) B cells were determined by flow cytometry after gating (G). The average values for activation of these B-cell subsets are indicated in panel C and reflect results for at least five mice per condition.

FIG. 4. B-cell activation after MNV infection. CD69 expression on $CD19^+$ B cells from the draining mesenteric lymph node (A) or spleen (B) after peroral infection with MNV. Each time point represents the average of at least five mice.

TABLE 1. B-cell activation after WNV infection in congenic deficient C57BL/6 mice[a]

Mouse strain	% $CD19^+$ $CD69^+$		n
	ILN	Spleen	
Wild type (no virus)	5.5 ± 2.7	3.7 ± 1.6	7
Wild type (WNV)	64.0 ± 7.4	14.1 ± 3.9	16
IFN-$\alpha\beta R^{-/-}$	20.9 ± 5.0**	25.1 ± 5.5**	7
$TLR3^{-/-}$	54.5 ± 12.5**	14.7 ± 4.0	11
$MyD88^{-/-}$	50.4 ± 8.7**	11.4 ± 5.1	9
Class II $MHC^{-/-}$	51.4 ± 15.1**	15.4 ± 3.2	10
IFN-$\gamma^{-/-}$	65.6 ± 3.8	11.6 ± 1.8	3
$IL-6^{-/-}$	69.3 ± 1.7	20.3 ± 5.4	8
$C3^{-/-}$	63.9 ± 11.4	15.6 ± 13.5	7
$IRF-3^{-/-}$	71.6 ± 12.9	21.3 ± 2.7	4
$IRF-7^{-/-}$	89.3 ± 1.5**	66.7 ± 2.2	7

[a] Wild-type or congenic deficient C57BL/6 mice were infected with 10^2 PFU of WNV-NY. ILN cells and splenocytes were harvested at days 3 and 4, respectively, and stained with anti-CD19 and anti-CD69 antibodies. The data are expressed as the percentage of $CD19^+$ B cells that coexpressed CD19 ± the standard deviation. n indicates the number of individual mice tested, and ** indicates statistically significant differences ($P < 0.01$) compared to WNV-infected wild-type mice.

expression of CD69 on B cells. Thus, individual genetic deficiencies in proteins that contribute to induction of IFN responses could not account for the majority of the early activation phenotype. More likely, multiple pathogen recognition receptors and signaling pathways coordinate the early IFN response in the draining ILN after WNV, resulting in B-cell activation.

Although components of the type I IFN response regulated early B-cell activation in the ILN, we hypothesized that other cytokines or humoral factors that modulate B cells might independently regulate activation. To evaluate this, we again assayed early B-cell activation after WNV infection in IFN-$\gamma^{-/-}$, $IL-6^{-/-}$, and $C3^{-/-}$ mice. Mice deficient in IFN-γ, IL-6, or the central complement component C3 showed high levels of CD69 expression on B cells that were equivalent to levels seen in wild-type mice. Mice deficient in class II MHC molecules had only a modest decrease in CD69 expression on B cells, suggesting that the early activation is largely T cell independent, as was observed for rotavirus (7).

Antigen specificity of early activated B cells. Maturation of surface IgM^+ naive B cells into high-affinity antigen-specific B cells (34) usually requires antigen stimulation in the context of costimulatory signals (e.g., CD40 or complement receptor 2) and $CD4^+$ T-cell help. Indeed, for WNV-NY infection, accumulation of antigen-specific IgG in serum was delayed and blunted in class II $MHC^{-/-}$, $CD4^{-/-}$, and $CD40^{-/-}$ mice (49, 50). Given the phenotype of rapid B-cell activation in the draining LN, we questioned whether this translated directly into an antigen-specific IgM response. To define the kinetics of the antigen-specific B-cell response in the ILN, B cells were harvested at day 3 and day 7 and tested in IgM ELISPOT assays against WNV envelope (E) protein or a nonspecific protein, ovalbumin (Fig. 5B). Despite the high degree of B-cell activation, we could not detect reliably any WNV-specific IgM-producing B cells (limit of detection, $1/10^6$ cells) at day 3. However, by day 7, IgM-producing B cells in the ILN showed antigen specificity for WNV (Fig. 5A) ($P < 0.01$).

icant ($P < 0.01$) reduction in B-cell activation in the ILN at 3 days after WNV infection (Table 1). Analogously, mice deficient in the TLR-7 and -8 adaptor molecule MyD88 also showed modest reductions in B-cell activation ($P < 0.05$). In contrast, deficiencies of the transcriptional activators IRF-3 and IRF-7 revealed relatively normal or even slightly increased
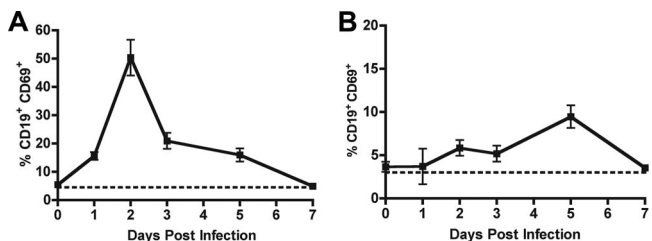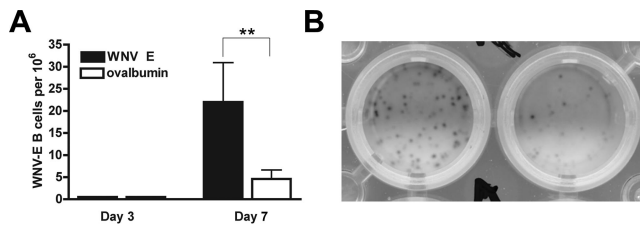
FIG. 5. Antigen-specific IgM ELISPOT in the ILN after WNV infection. A. Three or 7 days after infection with WNV, cells from the ILN were harvested and analyzed using an IgM ELISPOT against specific (WNV E protein) or nonspecific (ovalbumin) protein. The data are expressed as the number of antigen-specific B cells producing IgM per 10^6 cells and are averages of at least six mice per time point. B. A digital photographic example of an ELISPOT from B cells harvested at day 7 after WNV infection. The left well represents B cells that recognize WNV-E, and the right well represents nonspecific B cells that bind ovalbumin.

LN macrophages do not modulate B-cell activation after WNV infection. Recently, a novel model of viral antigen delivery to the draining LN leading to B-cell activation has been proposed: soluble virus enters the lymphatic channels directly

and transits to the LN through $CD169^+$ subcapsular sinus macrophages (25). To test whether LN macrophages contribute directly to B-cell activation after WNV infection, these cells were depleted after footpad injection of clodronate liposomes prior to virus infection (25). To confirm depletion, ILN cells were analyzed for expression of the myeloid cell markers F4/80, CD11b, CD11c, and CD169 7 days after liposome injection. As expected, treatment with clodronate-containing liposomes significantly depleted LN $F4/80^+$ and $CD169^+$ macrophages (Fig. 6A); in contrast, and as reported elsewhere (16), only slight reductions in splenic $F4/80^+$ macrophages were observed, and no effect was observed on lymphocyte populations (data not shown). After confirming depletion, we assessed B-cell activation after WNV-NY infection. Importantly, clodronate treatment in the absence of WNV infection did not induce expression of CD69 on B cells (data not shown). However, and in contrast to that observed previously with fixed inactivated vesicular stomatitis virus (VSV) (25), at day 3, there was a marked increase in the percentage of $CD19^+$ $CD69^+$ B cells in the ILN (Fig. 6B) ($P < 0.001$) and spleen
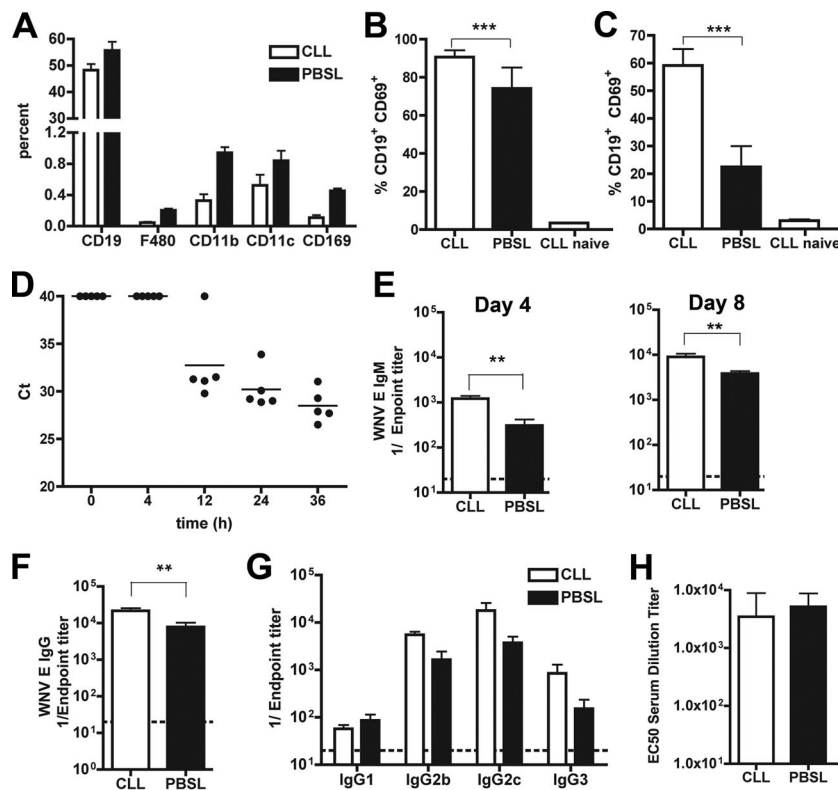

FIG. 6. Effects of LN macrophage depletion on B-cell activation and humoral response after WNV infection. Mice were treated with clodronate- or PBS-containing liposomes (CLL or PBSL, respectively) 1 week prior to infection with WNV-NY. A. Evidence of depletion of $F4/80^+$ and $CD169^+$ macrophages in the ILN by clodronate liposomes immediately prior to infection. Samples were processed by multicolor flow cytometry. Depletion with clodronate-containing liposomes reduced the number of $F4/80^+$ and $CD169^+$ macrophages by 78 and 76%, respectively. B and C. Effect of clodronate or PBS liposomes on B-cell activation as judged by CD69 expression after WNV infection in the ILN (B) and spleen (C). Cells were processed 3 (ILN) or 4 (spleen) days after infection. D. Time course of appearance of WNV RNA in the draining LN as judged by fluorogenic quantitative reverse transcription-PCR. The data are expressed as Ct values, where a value of 40 is considered negative. E and F. Effect of clodronate on WNV-specific IgM (E) and IgG (F) titers at days 4 and 8 after infection. Data are expressed as reciprocal log endpoint titers after regression analysis and reflect at least eight mice per group. G. IgG subclass analysis after clodronate- or PBS-liposome treatment. Samples were from day 8 after infection. No statistically significant differences were observed. H. Relative neutralizing activity of serum from mice treated with clodronate or PBS liposomes at day 8 after WNV infection. Samples were analyzed using a previously described reporter virus particle assay on Raji-DC-SIGN-R cells (40). Data are expressed as the EC_{50} titer (concentration at which 50% neutralization occurs) and reflect results for five mice per group. Asterisks represent statistically significant differences (**, $P < 0.01$; ***, $P < 0.001$).
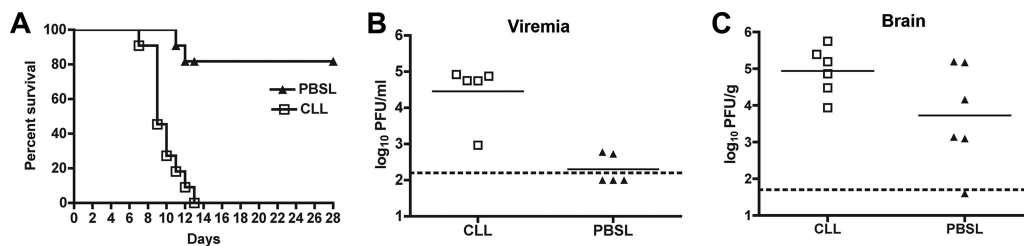
FIG. 7. Effects of LN macrophage depletion on WNV pathogenesis. Mice were treated with clodronate- or PBS-containing liposomes (CLL or PBSL, respectively) as described above and then infected with 10^2 PFU of WNV-NY. Animals were monitored for survival ($n = 11$ per group; $P < 0.0001$) (A) or viral burden as measured by plaque assay from serum at day 3 (B) or brain at day 8 (C) after infection. The dotted lines indicate the limit of sensitivity of the assay.

(Fig. 6C) ($P < 0.0001$) after WNV-NY infection, suggesting that macrophages were not required for efficient delivery of virus or activation of B cells. Whereas soluble VSV antigen trafficked rapidly to the LN within 2 h of inoculation (25), WNV RNA was not detected by fluorogenic quantitative reverse transcription-PCR in either the draining popliteal or ILN until 12 h after inoculation (Fig. 6D and data not shown), suggesting a round of viral replication in the skin may be required prior to LN entry. Taken together, our data suggest that LN macrophages are not required for rapid and early activation of B cells.

To assess whether macrophage depletion in the LN instead modulated the transition to adaptive B-cell responses, we measured WNV-specific serum IgM and IgG levels by enzyme-linked immunosorbent assay at days 4 and 8 after infection. In comparison to PBS liposome-treated mice, clodronate liposome-treated mice developed slightly higher levels of WNV-specific IgM at day 4 (Fig. 6E) (fourfold; $P < 0.01$). By day 8, clodronate-treated mice also sustained moderately higher levels of WNV-specific IgM (Fig. 6E) ($P < 0.01$) and IgG (Fig. 6F) ($P < 0.01$) compared to infected mice treated with PBS liposomes. Although clodronate-treated mice had robust antibody titers, macrophage depletion could affect isotype switching or maturation of B cells. However, at day 8, clodronate liposome-treated and control PBS liposome-treated mice showed similar IgG subclass and neutralizing activity profiles (Fig. 6G and H). Thus, depletion of macrophages in the draining LN after WNV does not severely disrupt the kinetics or quality of a functional antibody response.

One possible explanation as to why moderately increased levels of WNV-specific antibody were observed in clodronate liposome-treated mice is that these animals propagated more WNV. Higher WNV-specific antibody titers were observed previously in IFN-$\gamma^{-/-}$ (48) and IRF-3$^{-/-}$ (14) mice, which replicate WNV to greater levels in peripheral tissues. Moreover, systemic depletion of macrophages in outbred mice resulted in increased viremia and mortality after infection with an Israeli WNV isolate (4). To address this, we evaluated mice treated locally with clodronate liposomes for changes in viral burden and survival. Notably, mice depleted of ILN macrophages were more vulnerable to lethal WNV-NY infection, with a 100% mortality rate at day 10 after inoculation with 10^2 PFU of virus compared to a 18% mortality rate of PBS-liposome-treated mice (Fig. 7A) ($P < 0.0001$). Consistent with the increased lethality, clodronate-treated mice had higher levels of virus in the serum and brain (Fig. 7B and C) ($P < 0.01$).

Taken together, our data suggest that LN macrophage depletion associated with clodronate liposome treatment does not affect B-cell responses but rather enhances susceptibility through an antibody-independent mechanism.

DISCUSSION

In this report, we characterized the early steps of B-cell activation in the draining LN after WNV infection. Subcutaneous inoculation with a low dose of replicating WNV resulted in massive polyclonal B-cell activation in the LN within days of infection. Activation was dependent on IFN-α/βR signaling and partially dependent on the upstream pathogen recognition receptor and signaling components, such as TLR3 and MyD88. Despite global activation of B cells in the draining LN at day 3 after infection, IgM-producing WNV E protein-specific B cells were not detected until day 7. Our data suggest that WNV induces extensive IFN-α/β-dependent local and early polyclonal B-cell activation in the draining LN; however, this does not regulate the early antigen-specific antibody response that restricts infection.

Prior studies suggested that the early IgM response against WNV limited dissemination and lethality (18). Based on this, we hypothesized that draining LN B cells might produce WNV-specific antibody that limited spread. Indeed, we observed extensive activation of mature B cells in the ILN at early time points after WNV infection. This activation, however, was polyclonal, as nearly 70% of CD19$^+$ B cells were activated 3 days after infection, and in comparison, WNV-specific B cells in the ILN were not detected until 7 days after infection. Consistent with this, and confirming the antigen-independent nature of the stimulus, a similar degree of B-cell activation was observed after WNV infection in HELMET mice that transgenically express a single B-cell receptor for hen egg lysozyme. Parallel peroral infection studies with MNV, a member of the *Caliciviridae* family of positive-sense RNA viruses, induced a similar level and kinetics of B-cell activation in the draining mesenteric LN. Thus, polyclonal B-cell activation in the draining LN as observed with WNV infection may be a more general phenomenon following infection by viruses that rapidly replicate and cause disease. Indeed, our studies agree with recent reports that show polyclonal B-cell activation in mice after infection with rotavirus and influenza virus (6, 13).

Although viruses can induce B-cell activation soon after infection, the functional significance remains incompletely understood. B-cell activation has been hypothesized as important

for the production of natural antibody (36), the transition to mature B-cell populations (5), or possibly enhancing direct innate immune function by increasing surface expression of molecules that engage and activate $\gamma\delta$ T-cell or NK cells (11). Our experiments demonstrate that despite most of the CD19$^+$ cells in the draining LN showing an activation phenotype at day 3, no appreciable increase in antigen-specific B cells occurred. These results are consistent with a recent study with influenza virus that suggested that innate immune activation inhibits the ability of LN B cells to clonally expand following B-cell receptor stimulation (11). Thus, the early IgM response against WNV at day 4 that limits viremia and dissemination to distant sites (18) may be produced by B-1 cells that are located primarily in peritoneal and pleural cavities, or by marginal zone B cells in the spleen, and not by those in the draining LN.

Besides upregulating the fraction of B cells in the LN that become activated, we observed an increase in the total number of activated B cells within days of WNV infection. Experiments that analyzed expression of the cell proliferation-specific antigen Ki-67 revealed no significant change in B-cell proliferation. This suggests that B-cell hyperplasia in the ILN is likely due to retention of trafficking B cells that become activated locally. Although further studies are warranted, chemokine-directed signals (either B-cell extrinsic production of chemokines or B-cell intrinsic expression of chemokine receptors) may promote accumulation of activated B cells in the draining LN. Indeed, CCRL2 mRNA is upregulated in LN B cells after influenza virus infection, and significant changes in B-cell migratory patterns were observed with specific chemokines, including CCL19, CCL20, CCL21, and CXCL12 (11). Once B cells enter the ILN, CD69 expression may block exit from the LN by inhibiting responsiveness to the sphingosine 1-phosphate receptor 1 (47).

IFN-α/β produced during viral infection links innate and adaptive immune responses through direct stimulation of B and T cells (13, 21) and by enhancing antigen presentation (28). Our experiments suggest a strict requirement for IFN-α/β and polyclonal B-cell activation after WNV infection in the draining LN, results that agree with recent studies with influenza virus (11, 13), Semliki Forest virus (3), and VSV (21). Interestingly, experiments with a neutralizing IFN-α/βR MAb showed that treatment even 2 days after infection still abolished B-cell activation, suggesting that a sustained IFN-α/β signal is required to maintain B cells in the activated state or retain cells in the LN. Consistent with this, B-cell activation in the regional LN after WNV or MNV infection is transient, and CD69 expression rapidly returns to baseline a few days later, correlating with decreases in systemic and LN IFN-α/β levels (S. Daffis and M. Diamond, unpublished data).

In wild-type mice, a smaller fraction of splenic B cells expressed activation markers compared to the draining LN. Quite unexpectedly, and in contrast to the LN, an increase in B-cell activation in the spleen of IFN-α/βR$^{-/-}$ mice after WNV-MAD infection was observed. This increase could be the result of higher viral titers in the spleens in the IFN-α/βR$^{-/-}$ mice, since this less-virulent WNV strain has very low viral burden (42) or B-cell activation in the spleens of wild-type mice (W. Purtha and M. Diamond, unpublished data). Experiments with the anti-IFN-α/βR antibody, however, suggest that type I IFN-α/β signaling may indeed have a paradoxical inhib-itory effect on polyclonal B-cell activation in the spleen. Although pretreatment of mice with the neutralizing IFN-α/βR MAb resulted in augmented B-cell activation in the spleen at day 3 after infection, addition of MAb only 12 h postinfection did not increase splenic B-cell activation. One possible explanation is that systemic IFN-α/β that accumulates soon after infection modulates splenic B cells and inhibits polyclonal activation. It is not due a difference in viral burden in the spleen, as pretreatment or treatment 12 h postinfection of mice with the MAR-1 MAb results in equivalently elevated splenic viral burden (S. Daffis and M. Diamond, unpublished results). It remains unclear why B cells in the regional LN and spleen respond differently to IFN-α/β, although it may be due to distinct cytokine environments, B-cell subsets, and architecture with respect to the site of infection. We speculate that splenic B cells may respond differently to IFN-α/β to allow clonal expansion and maturation of antigen-specific antibody responses.

As B cells localize to the follicles in the interior of the LN, virus or viral antigen likely is presented after association with infected dendritic cells or by subcapsular macrophages that process lymphatic fluid contents (25). In contrast to that observed with fixed VSV antigen (25), B cells were highly activated in the draining LN despite extensive depletion of macrophages. Moreover, depletion of LN macrophages with clodronate liposomes did not alter WNV-specific antibody titers, isotype switching, or neutralizing activity. Nonetheless, depletion of LN macrophages did adversely affect WNV pathogenesis, as higher viral burdens and lethality were observed; these latter results are consistent with those of a prior study that showed that systemic depletion of macrophages causes more severe WNV infection (4). Although more detailed studies are required, macrophages may inhibit WNV infection due to specific innate immune functions, including secretion of antiviral and immunomodulatory cytokines and phagocytosis of opsonized infectious virus.

The early immune response to viruses involves the coordination of different immune cell types and humoral components. Soon after WNV infection, activated B cells accumulate in the draining LN via a type I IFN-α/βR-dependent mechanism which does not require translocation of antigen by CD169$^+$ subcapsular macrophages. These activated B cells, however, are not antigen specific or responsible for the early IgM response that controls WNV dissemination. Future studies will be directed at evaluating their role in innate immune system function and priming and how this leads to rapid control of viral dissemination.

REFERENCES

1. **Adachi, O., T. Kawai, K. Takeda, M. Matsumoto, H. Tsutsui, M. Sakagami, K. Nakanishi, and S. Akira.** 1998. Targeted disruption of the MyD88 gene results in loss of IL-1- and IL-18-mediated function. Immunity **9:**143–150.
2. **Alexopoulou, L., A. C. Holt, R. Medzhitov, and R. A. Flavell.** 2001. Recognition of double-stranded RNA and activation of NF-κB by Toll-like receptor 3. Nature **413:**732–738.

3. **Alsharifi, M., M. Lobigs, M. Regner, E. Lee, A. Koskinen, and A. Mull-bacher.** 2005. Type I interferons trigger systemic, partial lymphocyte activation in response to viral infection. J. Immunol. **175:**4635–4640.

4. **Ben-Nathan, D., I. Huitinga, S. Lustig, N. van Rooijen, and D. Kobiler.** 1996. West Nile virus neuroinvasion and encephalitis induced by macrophage depletion in mice. Arch. Virol. **141:**459–469.

5. **Bernasconi, N. L., E. Traggiai, and A. Lanzavecchia.** 2002. Maintenance of serological memory by polyclonal activation of human memory B cells. Science **298:**2199–2202.

6. **Blutt, S. E., S. E. Crawford, K. L. Warfield, D. E. Lewis, M. K. Estes, and M. E. Conner.** 2004. The VP7 outer capsid protein of rotavirus induces polyclonal B-cell activation. J. Virol. **78:**6974–6981.

7. **Blutt, S. E., K. L. Warfield, D. E. Lewis, and M. E. Conner.** 2002. Early response to rotavirus infection involves massive B cell activation. J. Immunol. **168:**5716–5721.

8. **Byrne, S. N., G. M. Halliday, L. J. Johnston, and N. J. King.** 2001. Interleukin-1β but not tumor necrosis factor is involved in West Nile virus-induced Langerhans cell migration from the skin in C57BL/6 mice. J. Investig. Dermatol. **117:**702–709.

9. **Carrasco, Y. R., and F. D. Batista.** 2007. B cells acquire particulate antigen in a macrophage-rich area at the boundary between the follicle and the subcapsular sinus in the lymph node. Immunity **27:**160–171.

10. **Catron, D. M., A. A. Itano, K. A. Pape, D. L. Mueller, and M. K. Jenkins.** 2004. Visualizing the first 50 hr of the primary immune response to a soluble antigen. Immunity **21:**341–347.

11. **Chang, W. L., E. S. Coro, F. C. Rau, Y. Xiao, D. J. Erle, and N. Baumgarth.** 2007. Influenza virus infection causes global respiratory tract B cell response modulation via innate immune signals. J. Immunol. **178:**1457–1467.

12. **Circolo, A., G. Garnier, W. Fukuda, X. Wang, T. Hidvegi, A. J. Szalai, D. E. Briles, J. E. Volanakis, R. A. Wetsel, and H. R. Colten.** 1999. Genetic disruption of the murine complement C3 promoter region generates deficient mice with extrahepatic expression of C3 mRNA. Immunopharmacology **42:**135–149.

13. **Coro, E. S., W. L. Chang, and N. Baumgarth.** 2006. Type I IFN receptor signals directly stimulate local B cells early following influenza virus infection. J. Immunol. **176:**4343–4351.

14. **Daffis, S., M. A. Samuel, B. C. Keller, M. Gale, Jr., and M. S. Diamond.** 2007. Cell-specific IRF-3 responses protect against West Nile virus infection by interferon-dependent and -independent mechanisms. PLoS Pathog. **3:**e106.

15. **Dalton, D. K., S. Pitts-Meek, S. Keshav, I. S. Figari, A. Bradley, and T. A. Stewart.** 1993. Multiple defects of immune cell function in mice with disrupted interferon-gamma genes. Science **259:**1739–1742.

16. **Delemarre, F. G., N. Kors, G. Kraal, and N. van Rooijen.** 1990. Repopulation of macrophages in popliteal lymph nodes of mice after liposome-mediated depletion. J. Leukoc. Biol. **47:**251–257.

17. **Diamond, M. S., B. Shrestha, A. Marri, D. Mahan, and M. Engle.** 2003. B cells and antibody play critical roles in the immediate defense of disseminated infection by West Nile encephalitis virus. J. Virol. **77:**2578–2586.

18. **Diamond, M. S., E. M. Sitati, L. D. Friend, S. Higgs, B. Shrestha, and M. Engle.** 2003. A critical role for induced IgM in the protection against West Nile virus infection. J. Exp. Med. **198:**1853–1862.

19. **Ebel, G. D., A. P. Dupuis II, K. Ngo, D. Nicholas, E. Kauffman, S. A. Jones, D. Young, J. Maffei, P. Y. Shi, K. Bernard, and L. D. Kramer.** 2001. Partial genetic characterization of West Nile virus strains, New York State, 2000. Emerg. Infect. Dis. **7:**650–653.

20. **Eriksson, K., I. Nordstrom, P. Horal, S. Jeansson, B. Svennerholm, A. Vahlne, J. Holmgren, and C. Czerkinsky.** 1992. Amplified ELISPOT assay for the detection of HIV-specific antibody-secreting cells in subhuman primates. J. Immunol. Methods **153:**107–113.

21. **Fink, K., K. S. Lang, N. Manjarrez-Orduno, T. Junt, B. M. Senn, M. Holdener, S. Akira, R. M. Zinkernagel, and H. Hengartner.** 2006. Early type I interferon-mediated signals on B cells specifically enhance antiviral humoral responses. Eur. J. Immunol. **36:**2094–2105.

22. **Gerdes, J., H. Lemke, H. Baisch, H. H. Wacker, U. Schwab, and H. Stein.** 1984. Cell cycle analysis of a cell proliferation-associated human nuclear antigen defined by the monoclonal antibody Ki-67. J. Immunol. **133:**1710–1715.

23. **Hardy, R. R., and K. Hayakawa.** 2001. B cell development pathways. Annu. Rev. Immunol. **19:**595–621.

24. **Honda, K., H. Yanai, H. Negishi, M. Asagiri, M. Sato, T. Mizutani, N. Shimada, Y. Ohba, A. Takaoka, N. Yoshida, and T. Taniguchi.** 2005. IRF-7 is the master regulator of type-I interferon-dependent immune responses. Nature **434:**772–777.

25. **Junt, T., E. A. Moseman, M. Iannacone, S. Massberg, P. A. Lang, M. Boes, K. Fink, S. E. Henrickson, D. M. Shayakhmetov, N. C. Di Paolo, N. van Rooijen, T. R. Mempel, S. P. Whelan, and U. H. von Andrian.** 2007. Subcapsular sinus macrophages in lymph nodes clear lymph-borne viruses and present them to antiviral B cells. Nature **450:**110–114.

26. **Keller, B. C., B. L. Fredericksen, M. A. Samuel, R. E. Mock, P. W. Mason, M. S. Diamond, and M. Gale, Jr.** 2006. Resistance to alpha/beta interferon is a determinant of West Nile virus replication fitness and virulence. J. Virol. **80:**9424–9434.

27. **Kopf, M., H. Baumann, G. Freer, M. Freudenberg, M. Lamers, T. Kishimoto, R. Zinkernagel, H. Bluethmann, and G. Kohler.** 1994. Impaired immune and acute-phase responses in interleukin-6-deficient mice. Nature **368:**339–342.

28. **Le Bon, A., G. Schiavoni, G. D'Agostino, I. Gresser, F. Belardelli, and D. F. Tough.** 2001. Type I interferons potently enhance humoral immunity and can promote isotype switching by stimulating dendritic cells in vivo. Immunity **14:**461–470.

29. **Loder, F., B. Mutschler, R. J. Ray, C. J. Paige, P. Sideras, R. Torres, M. C. Lamers, and R. Carsetti.** 1999. B cell development in the spleen takes place in discrete steps and is determined by the quality of B cell receptor-derived signals. J. Exp. Med. **190:**75–89.

30. **Lopes-Carvalho, T., and J. F. Kearney.** 2004. Development and selection of marginal zone B cells. Immunol. Rev. **197:**192–205.

31. **Lopez-Cabrera, M., A. G. Santis, E. Fernandez-Ruiz, R. Blacher, F. Esch, P. Sanchez-Mateos, and F. Sanchez-Madrid.** 1993. Molecular cloning, expression, and chromosomal localization of the human earliest lymphocyte activation antigen AIM/CD69, a new member of the C-type animal lectin superfamily of signal-transmitting receptors. J. Exp. Med. **178:**537–547.

32. **Madsen, L., N. Labrecque, J. Engberg, A. Dierich, A. Svejgaard, C. Benoist, D. Mathis, and L. Fugger.** 1999. Mice lacking all conventional MHC class II genes. Proc. Natl. Acad. Sci. USA **96:**10338–10343.

33. **McClellan, K. B., S. Gangappa, S. H. Speck, and H. W. T. Virgin.** 2006. Antibody-independent control of gamma-herpesvirus latency via B cell induction of anti-viral T cell responses. PLoS Pathog. **2:**e58.

34. **Mehlhop, E., K. Whitby, T. Oliphant, A. Marri, M. Engle, and M. S. Diamond.** 2005. Complement activation is required for induction of a protective antibody response against West Nile virus infection. J. Virol. **79:**7466–7477.

35. **Mombaerts, P., J. Iacomini, R. S. Johnson, K. Herrup, S. Tonegawa, and V. E. Papaioannou.** 1992. RAG-1-deficient mice have no mature B and T lymphocytes. Cell **68:**869–877.

36. **Ochsenbein, A. F., T. Fehr, C. Lutz, M. Suter, F. Brombacher, H. Hengartner, and R. M. Zinkernagel.** 1999. Control of early viral and bacterial distribution and disease by natural antibodies. Science **286:**2156–2159.

37. **Oliphant, T., G. E. Nybakken, S. K. Austin, Q. Xu, J. Bramson, M. Loeb, M. Throsby, D. H. Fremont, T. C. Pierson, and M. S. Diamond.** 2007. Induction of epitope-specific neutralizing antibodies against West Nile virus. J. Virol. **81:**11828–11839.

38. **Pape, K. A., D. M. Catron, A. A. Itano, and M. K. Jenkins.** 2007. The humoral immune response is initiated in lymph nodes by B cells that acquire soluble antigen directly in the follicles. Immunity **26:**491–502.

39. **Phan, T. G., I. Grigorova, T. Okada, and J. G. Cyster.** 2007. Subcapsular encounter and complement-dependent transport of immune complexes by lymph node B cells. Nat. Immunol. **8:**992–1000.

40. **Pierson, T. C., M. D. Sanchez, B. A. Puffer, A. A. Ahmed, B. J. Geiss, L. E. Valentine, L. A. Altamura, M. S. Diamond, and R. W. Doms.** 2005. A rapid and quantitative assay for measuring antibody-mediated neutralization of West Nile virus infection. Virology **346:**53–65.

41. **Qi, H., J. G. Egen, A. Y. Huang, and R. N. Germain.** 2006. Extrafollicular activation of lymph node B cells by antigen-bearing dendritic cells. Science **312:**1672–1676.

42. **Samuel, M. A., and M. S. Diamond.** 2005. Alpha/beta interferon protects against lethal West Nile virus infection by restricting cellular tropism and enhancing neuronal survival. J. Virol. **79:**13350–13361.

43. **Samuel, M. A., and M. S. Diamond.** 2006. Pathogenesis of West Nile Virus infection: a balance between virulence, innate and adaptive immunity, and viral evasion. J. Virol. **80:**9349–9360.

44. **Sato, M., H. Suemori, N. Hata, M. Asagiri, K. Ogasawara, K. Nakao, T. Nakaya, M. Katsuki, S. Noguchi, N. Tanaka, and T. Taniguchi.** 2000. Distinct and essential roles of transcription factors IRF-3 and IRF-7 in response to viruses for IFN-alpha/beta gene induction. Immunity **13:**539–548.

45. **Sejvar, J. J.** 2006. The evolving epidemiology of viral encephalitis. Curr. Opin. Neurol. **19:**350–357.

46. **Sheehan, K. C., K. S. Lai, G. P. Dunn, A. T. Bruce, M. S. Diamond, J. D. Heutel, C. Dungo-Arthur, J. A. Carrero, J. M. White, P. J. Hertzog, and R. D. Schreiber.** 2006. Blocking monoclonal antibodies specific for mouse IFN-alpha/beta receptor subunit 1 (IFNAR-1) from mice immunized by in vivo hydrodynamic transfection. J. Interferon Cytokine Res. **26:**804–819.

47. **Shiow, L. R., D. B. Rosen, N. Brdickova, Y. Xu, J. An, L. L. Lanier, J. G. Cyster, and M. Matloubian.** 2006. CD69 acts downstream of interferon-alpha/beta to inhibit S1P1 and lymphocyte egress from lymphoid organs. Nature **440:**540–544.

48. **Shrestha, B., T. Wang, M. A. Samuel, K. Whitby, J. Craft, E. Fikrig, and M. S. Diamond.** 2006. Gamma interferon plays a crucial early antiviral role in protection against West Nile virus infection. J. Virol. **80:**5338–5348.

49. **Sitati, E., E. E. McCandless, R. S. Klein, and M. S. Diamond.** 2007. CD40-CD40 ligand interactions promote trafficking of CD8+ T cells into the brain and protection against West Nile virus encephalitis. J. Virol. **81:**9801–9811.

50. **Sitati, E. M., and M. S. Diamond.** 2006. CD4+ T-cell responses are required for clearance of West Nile virus from the central nervous system. J. Virol. **80:**12060–12069.

51. **Slifka, M. K., M. Matloubian, and R. Ahmed.** 1995. Bone marrow is a major

site of long-term antibody production after acute viral infection. J. Virol. **69:**1895–1902.

52. **Stevenson, P. G., and P. C. Doherty.** 1999. Non-antigen-specific B-cell activation following murine gammaherpesvirus infection is CD4 independent in vitro but CD4 dependent in vivo. J. Virol. **73:**1075–1079.

53. **Thomas, M. D., B. Srivastava, and D. Allman.** 2006. Regulation of peripheral B cell maturation. Cell. Immunol. **239:**92–102.

54. **Van Rooijen, N., and A. Sanders.** 1994. Liposome mediated depletion of macrophages: mechanism of action, preparation of liposomes and applications. J. Immunol. Methods **174:**83–93.

55. **Wobus, C. E., S. M. Karst, L. B. Thackray, K. O. Chang, S. V. Sosnovtsev, G. Belliot, A. Krug, J. M. Mackenzie, K. Y. Green, and H. W. Virgin.** 2004. Replication of norovirus in cell culture reveals a tropism for dendritic cells and macrophages. PLoS Biol. **2:**e432.